

archives  
of thermodynamics

Vol. 40(2019), No. 4, 103–128  
DOI: 10.24425/ather.2019.131430

## Modelling of back propagation neural network to predict the thermal performance of porous bed solar air heater

HARISH KUMAR GHRITLAHRE  
RADHA KRISHNA PRASAD\*

Mechanical Engineering Department, National Institute of Technology,  
Jamshedpur, 831014, Jharkhand, India

**Abstract** The objective of present work is to predict the thermal performance of wire screen porous bed solar air heater using artificial neural network (ANN) technique. This paper also describes the experimental study of porous bed solar air heaters (SAH). Analysis has been performed for two types of porous bed solar air heaters: unidirectional flow and cross flow. The actual experimental data for thermal efficiency of these solar air heaters have been used for developing ANN model and trained with Levenberg-Marquardt (LM) learning algorithm. For an optimal topology the number of neurons in hidden layer is found thirteen (LM-13). The actual experimental values of thermal efficiency of porous bed solar air heaters have been compared with the ANN predicted values. The value of coefficient of determination of proposed network is found as 0.9994 and 0.9964 for unidirectional flow and cross flow types of collector respectively at LM-13. For unidirectional flow SAH, the values of root mean square error, mean absolute error and mean relative percentage error are found to be 0.16359, 0.104235 and 0.24676 respectively, whereas, for cross flow SAH, these values are 0.27693, 0.03428, and 0.36213 respectively. It is concluded that the ANN can be used as an appropriate method for the prediction of thermal performance of porous bed solar air heaters.

**Keywords:** Solar air heater; Porous bed; Thermal performance; Artificial neural network; Levenberg-Marquardt algorithm

---

\*Corresponding Author. Email: rkprasad.me@nitjsr.ac.in<sup>b</sup>

## Nomenclature

$A_c$	– area of collector surface, m <sup>2</sup>
$a_i$	– input data
$b_j$	– bias
$C_p$	– specific heat, J/kgK
COV	– coefficient of variance
$G$	– solar irradiance, W/m <sup>2</sup>
$M$	– input parameters
$\dot{m}_f$	– mass flow rate of air, kg/s
MRE	– mean relative error
MSE	– mean square error
MAE	– mean absolute error
$N$	– output parameters
$\dot{Q}_c$	– rate of incident energy on the collector area, W
$\dot{Q}_u$	– rate of useful energy gained by air, W
RMSE	– root mean square error
$R$	– correlation coefficient
$R^2$	– coefficient of multiple determination
SSE	– sum square error
$T$	– temperature, K
$T_n$	– number of training data sets
$w_{ij}$	– weights
$X_A$	– actual value
$Y_P$	– predicted value

## Greek symbols

$\eta_{th}$	– thermal efficiency of collector
-------------	-----------------------------------

## Subscripts

$a$	– ambient air
$fi$	– inlet air
$fo$	– outlet air
$fm$	– mean air

## Abbreviations

ANN	– artificial neural networks
LM	– Levenberg-Marquardt
MLP	– multilayered perceptron
SAH	– solar air heater

## 1 Introduction

A solar air heater (SAH) is a special type of heat exchanger which absorbs solar radiations and transfers the absorbed thermal energy to the

flowing fluid (air). The heated air is used for space heating in commercial and residential buildings, particularly in colder regions (like northern and north – eastern regions of India) in winter where a significant amount of energy is required for heating. In addition to this it is used for crop drying, timber seasoning and various low temperature heating applications. The thermal efficiency of a solar air heater is usually low because of the low heat transfer coefficient between the heat transfer surface and the flowing air which results in higher heat losses to atmosphere [1,2]. In the past, artificial roughness on absorber plate of solar air heater [3–6] or packing porous materials as absorber in the SAHs ducts [7–14] have been employed to enhance its thermal efficiency. Packed bed solar air heater is one of the type of solar air heaters, in which incident solar radiations penetrate to a greater depth and are absorbed gradually depending on the density of packing material. Porous absorber has high heat transfer surface area density and hence high heat transfer rate resulting in an increase in thermal efficiency of the solar air heater.

A variety of designs of packed bed solar air heaters, such as slit- and-expanded aluminum foil matrix, wire screen matrices [7–9], glass beads [10], etc. have been suggested. By the use of screen matrix as a packing material the thermal efficiency of solar air heater can be enhanced [9]. In this design, solar radiation is absorbed in depth which results in relatively low temperature of absorber at top surface of the packing, which decreases the heat losses from the absorber to ambient air and hence, increases the thermal efficiency of the solar air heaters. The thermal performance enhancement of packed bed solar air heater depends on types of geometrical and thermophysical characteristics of packed bed materials [10–14].

The experimental study as well as the analytical study followed by the computational techniques, require a lot of time to arrive at an accurate result of a physical problem. The use of artificial neural networks (ANN), on the other hand, saves time and also provides key information patterns in a multidimensional information domain and, therefore, this technique has been becoming increasingly popular in science and engineering, especially in mechanical engineering applications in recent years. Many researchers have used ANN in the past; Kalogirou used ANN technique for performance prediction of renewable energy systems [15]. Kalogirou and Bojic applied ANN tool for prediction of energy consumption of passive solar building systems [16]. Yang *et al.* [17] have applied ANN technique to predict the optimal start time for heating system in building. Facao *et*

*al.* [18] used ANN for simulation of hybrid solar collectors. Ertunc and Hosoz applied ANN technique for analysis of a refrigeration system with an evaporative condenser [19]. Kalogirou used ANN technique for predicting the flat plate collector performance parameters [20]. Yilmaz and Atik used ANN for modeling of a cooling system with variable cooling capacity [21]. Sozen *et al.* applied ANN for determination of efficiency of flat-plate solar collectors [22]. Kurt *et al.* [23] have used artificial neural network technique for estimating thermal performance parameters of hot box type solar cooker. Yuhong and Wenxin used ANN to predict the frictional factor of open channel flow [24]. Caner *et al.* [25] and Benli [26] applied ANN model for investigation on thermal performance calculation of two types of solar air collectors. Dikmen *et al.* [27] structured artificial neural networks and adaptive neuro fuzzy inference system (ANFIS) models to predict the performance of evacuated tube solar collectors. Kalogirou *et al.* [28] implemented ANN tool for performance prediction of large solar systems. Ghritlahre and Prasad developed ANN model to estimate the performance of unidirectional flow solar air heater using optimal training function [29]. May *et al.* [31,32] studied the concept leading to selection of input variables for ANN model. Ghritlahre and Prasad [33–39] used ANN technique to predict the performances of various types of solar air heaters.

Though performance analysis of various types of solar air heaters are available in the above literature, however, very limited studies on application of artificial neural network for thermal performance prediction of porous bed solar air heaters are available in the literature. The optimal number of neurons in hidden layer have been selected randomly in the previous work, but in the present study the multilayer perceptron (MLP) model has been trained with optimal number of neurons in hidden layer [16] to find the best results, which are the novelties of this research work.

In view of the above, ANN model has been developed to predict the thermal performance of porous bed solar air heaters by using measured experimental data and the calculated values of performance parameters. Total 192 experimental data sample have been used. The 96 sample data, each for unidirectional flow and cross flow types porous bed solar air heaters have been taken and divided into three groups as training (80% data), validation (10% data) and testing (10% data). This multilayer perceptron neural model has been structured with a single hidden layer using seven parameters in input layer and one output parameter in output layer. Proposed MLP model has been trained with Levenberg-Marquardt (LM) learn-

ing algorithm to predict the thermal performances of porous bed solar air heaters. Predicted and measured values of thermal efficiencies have been compared. Comparisons of errors are evaluated *via* statistical error analysis according to model types and sample groups.

## 2 Material and method

### 2.1 Experimental study

Figure 1 shows schematic diagram of experimental system with two different flow configurations: unidirectional flow and cross flow. In unidirectional flow the directions of incident solar radiation and the flowing air in the porous bed are same whereas, in cross flow type these are perpendicular to each other. The detailed specifications of the porous absorbers used for the study have been given in Tab. 1. The exposed area of each of the solar collector test sections is 1.22 m×0.45 m. The absorber plates have been made of 24 gauge mild steel (MS) sheet painted with black board paint. A 3 mm thick glass sheet, as cover, has been used at top of each test section and bottom and sides are insulated with 6 cm thick glass wool supported by a 0.05 m plywood sheet. Each test section is connected with a wooden rectangular duct of 1.50 m×0.45 m×0.05 m size with bell-mouth entry for straightening the air flow to the test sections. Two types of wire screen matrices of the specifications as given in Tab. 1 have been considered in the present study.

The collectors have been tested as per ASHRAE 93-97 standards [1,2]. The experiments were conducted under clear sky condition at Roorkee (India) between 10:30 to 14:00 hours. A 2.5 kW centrifugal blower was used to induce air to the test sections. Six different mass flow rates of air in the range of 0.0100–0.0225 kg/s were considered for the collectors during the test. The intensity of incident solar radiation was measured by means of a pyranometer, connected to a digital microvoltmeter for direct display. Copper-constantan thermocouples (28 SWG) were used to measure the air temperatures of inlet and outlet of the test sections and the ambient temperature. The measurement of air flow rate through the test section has been accomplished by using orifice meters. Tests were conducted with two types of screen absorbers **A** and **B**, as given in Tab. 1. Total 192 data sample were taken from the experiments.

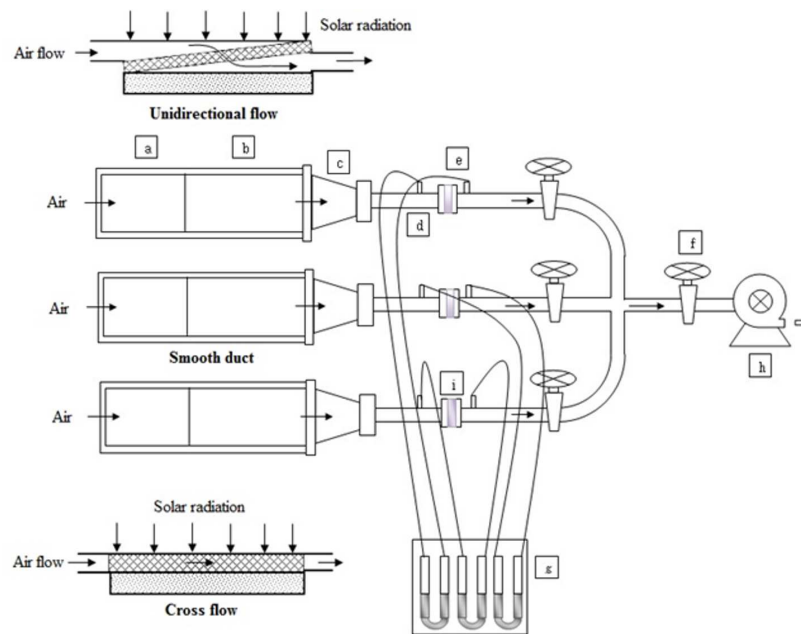


Figure 1: Schematic diagram of experimental setup [9]: a – entry section (flow straighteners), b – test section, c – exit section, d – galvanized iron (GI) pipe, e – pipe flange, f – control valve, g – U-tube manometer, h – centrifugal blower, i – orifice plate.

Table 1: Specification of the absorbers (screen matrices) [9].

Parameter	Absorber	
	Type A (Model I)	Type B (Model II)
Mesh no. ( $m^{-1}$ )	$0.045 \times 0.045$	$0.04 \times 0.04$
Wire diameter, bare (m)	$0.464 \times 10^{-3}$	$0.556 \times 10^{-3}$
Wire diameter, painted (m)	$0.480 \times 10^{-3}$	$0.582 \times 10^{-3}$
Screen thickness (m)	$0.90 \times 10^{-3}$	$1.15 \times 10^{-3}$
Mesh pitch (m)	$2.22 \times 10^{-3}$	$2.50 \times 10^{-3}$
Porosity	0.925	0.915

## 2.2 Performance evaluation of solar air heater

The performance of solar collector for heating air is represented by the term thermal efficiency which is defined as the ratio of solar energy gain to incident solar radiation on the collector exposed area [3,25,26].

Collector thermal efficiency is

$$\eta_{th} = \frac{\dot{Q}_u}{\dot{Q}_c}, \quad (1)$$

where  $\dot{Q}_u$  is the useful heat gain of the rate of heat transfer to working fluid (air) in the solar collector, and  $\dot{Q}_c$  is the rate of solar energy incident on the collector surface. The solar energy incident on the collector surface can be written as

$$\dot{Q}_c = GA_c, \quad (2)$$

where  $G$  is the rate of incidence of solar radiations per unit area of the collector surface, and  $A_c$  is the collector area. The solar energy, absorbed by the absorber is transferred to the flowing air which is the useful energy gain by flowing air and is given as

$$\dot{Q}_u = \dot{m}_f C_p \Delta T_f = \dot{m}_f C_p (T_{fo} - T_{fi}), \quad (3)$$

where  $C_p$  is the specific heat,  $\dot{m}_f$  is the mass flow rate of air,  $T_{fo}$  and  $T_{fi}$  are the inlet and outlet temperature of air, respectively. Thus, the efficiency of solar collector for heating air is written as [1,2,29]

$$\eta_{th} = \frac{\dot{m}_f C_p (T_{fo} - T_{fi})}{GA_c}. \quad (4)$$

### 2.3 Artificial neural network

Artificial neural network (ANN) is a complex information processing system, which is structured from interconnected segmental processing elements, called neurons. These neurons find the input information from other sources and perform generally a nonlinear operation on the result and then give final results as output. ANN works in two ways, first learning and then storing the knowledge in interconnects called weights. The basic structure of artificial neurons is represented in Fig. 2. ANN is a simulation tool in Matlab [40] which can be used to estimate the values on the basis of input parameters, optimum topology and training processes. In feed forward networks, each product of input elements and weights are fed to summing junctions and is summed with bias of neurons as follows [30,33]:

$$X = \sum_{i=1}^n w_{ij} a_i + b_j, \quad (5)$$

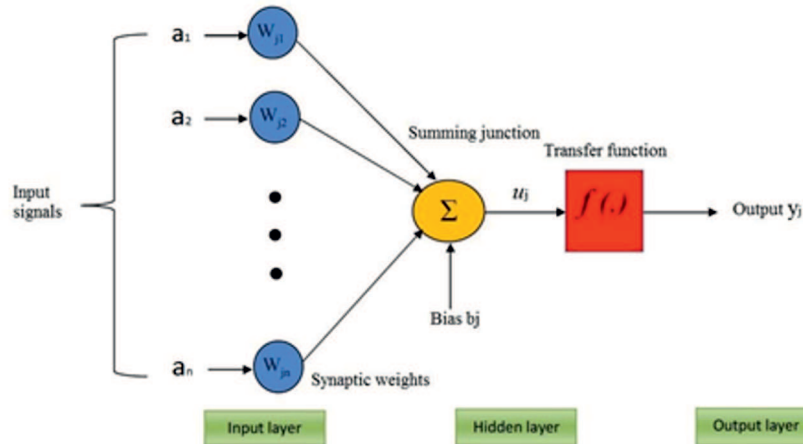


Figure 2: Basic structure of artificial neuron.

where  $n$  is the number of input signals. Then this sum  $X$  passes through transfer function  $F$  which generates an output

$$F(X) = u_j = F \left[ \sum_{i=1}^n w_{ij} a_i + b_j \right]. \quad (6)$$

The most used transfer functions in hidden layer are *tansig* and *logsig*. The nonlinear activation function which is widely used, is called as *sigmoid* function whose output lies between 0 and 1, and is given as

$$F(X) = \frac{1}{1 + e^{-X}}. \quad (7)$$

When negative values are found at input or output layer then the *tansig* transfer function is used, which is given as

$$F(X) = \frac{1 - e^{-2X}}{1 + e^{-2X}}. \quad (8)$$

The performance of different training processes is evaluated by mean square error (MSE), coefficient of variance (COV) and coefficient of determination ( $R^2$ ), and these factors are formulated as:

mean square error

$$\text{MSE} = \frac{1}{n} \sum_{i=1}^n (X_{A,i} - Y_{P,i})^2, \quad (9)$$



coefficient of variance

$$\text{COV} = \frac{RMSE}{\frac{1}{n} \sum_{i=1}^n Y_{P,i}} \times 100, \quad (10)$$

coefficient of determination

$$R^2 = 1 - \frac{\sum_{i=1}^n (X_{A,i} - Y_{P,i})^2}{\sum_{i=1}^n Y_{P,i}^2}, \quad (11)$$

where  $X_A$  and  $Y_P$  are actual and predicted value, respectively, and  $n$  is the numbers of data.

### 3 Results and discussion

In the present work, two different types of solar air heater have been used for evaluation of their thermal performance. These SAHs are unidirectional flow and cross flow types. The porous absorber of two different specifications **A** and **B**, as given Tab. 1, have been used in the SAHs [9]. The experiments have been conducted for various mass flow rates from 0.0100 to 0.0225 kg/s.

The thermal efficiency of both types of porous bed SAH was calculated from the experimental data. Figure 3 shows the variation of thermal efficiency with time. From this graph, we find that thermal efficiency first increases with time and after 12:30 hours, at which the solar irradiance is approximately maximum, it starts decreasing for both types of SAHs. The maximum efficiency is found 50.58% for unidirectional flow and 48.95% cross flow SAH. In addition to this, it is found that the thermal efficiency of type **B** absorber is higher than type **A** for both of the SAHs. This is due to the high transfer rate from the porous absorber to the air, owing to the lower porosity of this absorber.

The variation of mass flow rate of air with thermal efficiency of both SAHs for Type **A** absorber, has been shown in Fig. 4. This figure shows that the maximum thermal efficiency is 55.1% and 50.93% for both unidirectional and cross flow type porous bed SAH respectively for air mass flow rate of 0.0225 kg/s. At this particular mass flow rate unidirectional flow SAH has 7.45% higher efficiency as compared to cross flow type SAH. On the other hand, at lower mass flow rate the unidirectional flow has 9.40% higher efficiency than cross flow type SAH. Unidirectional flow porous bed solar air heater is more efficient than the cross flow type solar air heater.

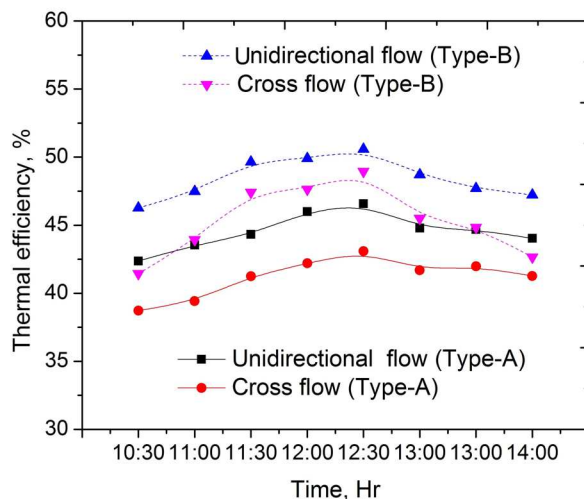


Figure 3: Variation of thermal efficiency with time (for  $\dot{m} = 0.0100$  kg/s.)

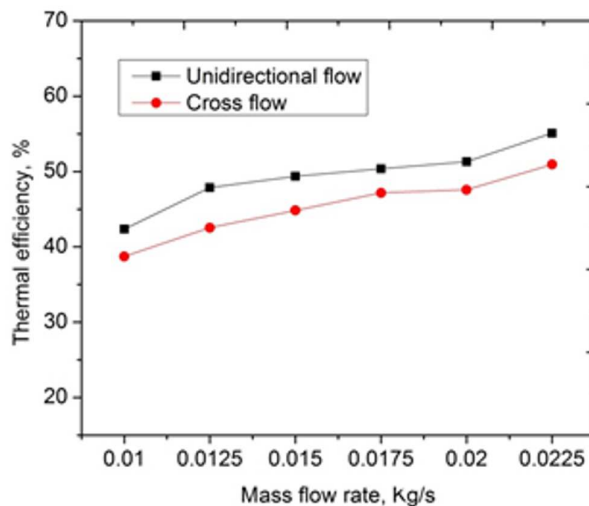


Figure 4: Variation of thermal efficiency with mass flow rate of porous bed SAHs for type A absorber.

### 3.1 Analysis of the experimental data using artificial neural network

In the presented work, first the number of data sets which affects the performance of the system has been selected. The three layers network: the

input variables of input layer, hidden layer and output variable of output layer are shown in Fig. 5. Five input variables in input layer are, inlet temperature of air,  $T_{fi}$ , air mean temperature,  $T_{fm}$ , ambient temperature  $T_a$ , solar irradiance,  $G$ , and mass flow rate of air,  $\dot{m}_f$ , that affect the thermal performance of porous bed solar air heaters. The values of these five variables are taken from experimental studies. Total seven input variables including type of absorber and the time of measuring experimental data have been selected (Fig. 5) in the input layer [31,32]. The output variable is thermal efficiency,  $\eta_{th}$ , of porous bed solar air heater, which is used in output layer. Range of variables in input and output layers for unidirectional flow and cross flow porous bed solar air heaters for ANN model have been given in Tab. 2.

Table 2: Range of input and output parameters for proposed ANN model.

Parameters	Range	
	Unidirectional flow SAH	Cross flow SAH
<i>Input</i>		
Mass flow rate of air, $m_f$ (kg/sec)	0.0100–0.0225	0.0100–0.0225
Ambient air temp., $T_a$ ( $^{\circ}$ C)	28.20–34.80	28.20–34.80
Inlet temp. of air, $T_{fi}$ ( $^{\circ}$ C)	29.00–37.33	29.00–37.33
Mean temp. of air, $T_{fm}$ ( $^{\circ}$ C)	33.84–49.03	33.44–47.99
Solar irradiance, $G$ ( $W/m^2$ )	682.75–963.35	682.75–963.35
<i>Output</i>		
Thermal efficiency ( $\eta_{th}$ )	42.37–64.17	38.72–59.30

Before developing the ANN model, the input/output sample data must be normalized between -1 and 1 for accuracy of prediction. The normalized value,  $Y_{norm}$ , for each raw input/output data set,  $Y_i$ , was calculated as

$$Y_{norm} = \frac{Y_i - Y_{\min}}{Y_{\max} - Y_{\min}} (\text{High}_{value} - \text{Low}_{value}) + \text{Low}_{value} , \quad (12)$$

where the high value and low value is 1 and -1, respectively.

In this study, the experimental data recorded for 12 days for both unidirectional flow and cross flow porous bed solar air heaters have been taken. Out of total 192 data, obtained from experiments, 96 data are for unidirectional flow and remaining 96 data for cross flow collector. In both flow types first 48 data is for the absorber type **A** and remaining 48 is for the absorber type **B**. Out of 192 data 96 and 96 samples are used separately for ANN modeling.

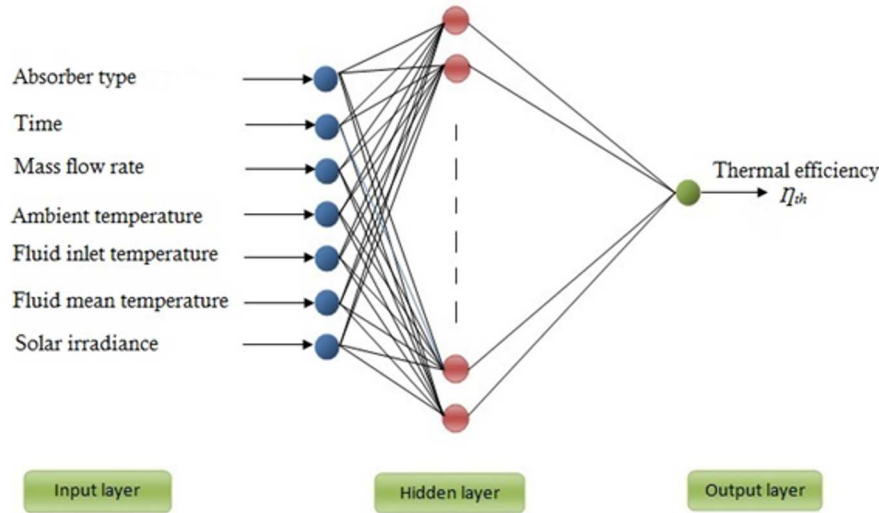


Figure 5: The structure of proposed ANN model.

The aim of the work is to predict the thermal performance of the porous bed solar air heater using ANN model. The computer program was performed by using Matlab 7.10.0 (2010a) [40] neural network tool (neural network fitting tool), in which 76 samples data are used for training, 10 samples data are used for cross validation and 10 samples are used for testing.

The trial and error method is adopted to select number of neurons in the hidden layer. However, some thumb rules are available in the literature for selection of number of neurons in hidden layer. One of them reported by Kalogirou and Bojic [16] to calculate the optimal number of neurons is

$$H = \frac{M + N}{2} + \sqrt{T_n}, \quad (13)$$

where  $M$  and  $N$  are input and output parameters respectively, and  $T_n$  is a number of training data sets.

Using formula (13), the number of neurons is obtained as 13, so on the basis of trial and error, 10–15 number of neurons have been selected in hidden layer to predict the output result accurately. For optimal result of hidden layer we use different number of hidden neurons in the network. Statistical training results such as mean square error (MSE),  $R^2$  and COV are shown in Tab. 3.

Table 3: The training results of different hidden neurons in LM learning algorithm.

Number of neurons	MSE	COV	$R^2$
Unidirectional flow			
LM-10	0.53167	1.40968	0.96808
LM-11	0.48088	1.33410	0.98024
LM-12	0.32362	1.10030	0.99166
LM-13	0.08130	0.55180	0.99524
LM-14	0.15206	0.75504	0.99126
LM-15	0.57269	1.46612	0.96441
Cross flow			
LM-10	0.06404	0.52754	0.99606
LM-11	0.05965	0.50980	0.99639
LM-12	0.05414	0.48549	0.99673
LM-13	0.04684	0.45241	0.99715
LM-14	0.07044	0.55404	0.99569
LM-15	0.19812	0.92899	0.98841

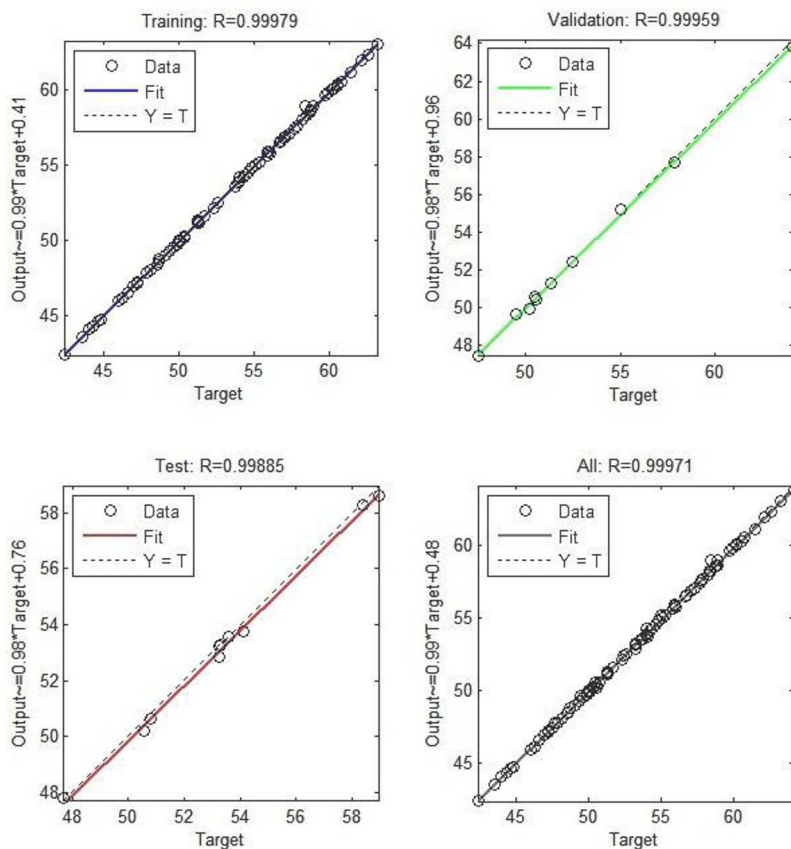
From Tab. 3, Levenberg-Marquardt (LM) algorithm with 13 neurons in hidden layer is found to be the most optimal network for both types of solar air heaters because maximum  $R^2$  and minimum MSE and COV values were obtained. In this study the number of neurons in the hidden layer has been chosen thirteen (LM-13) for both types of solar air heaters of ANN model. Due to the hyperbolic nature of nf-tool tan-sigmoid function is used for hidden layer and linear transfer function is used for the output layer.

In neural network, we use LM back propagation function. This function is a network training function that updates weight and bias values according to LM optimization method.

The parameters used in trainlm training process are shown below:

Training algorithm:	Levenberg-Marquardt (trainLM)
Performance Index:	mean square error (MSE)
Maximum number of epoch for training:	1000
Performance goal:	0
Maximum validation failure:	6
Minimum gradient error:	$1.00 \times 10^{-10}$
$\mu$ initial:	0.001
Maximum $\mu$ :	$1.00 \times 10^{+10}$
Decreasing factor $\mu$ :	0.1

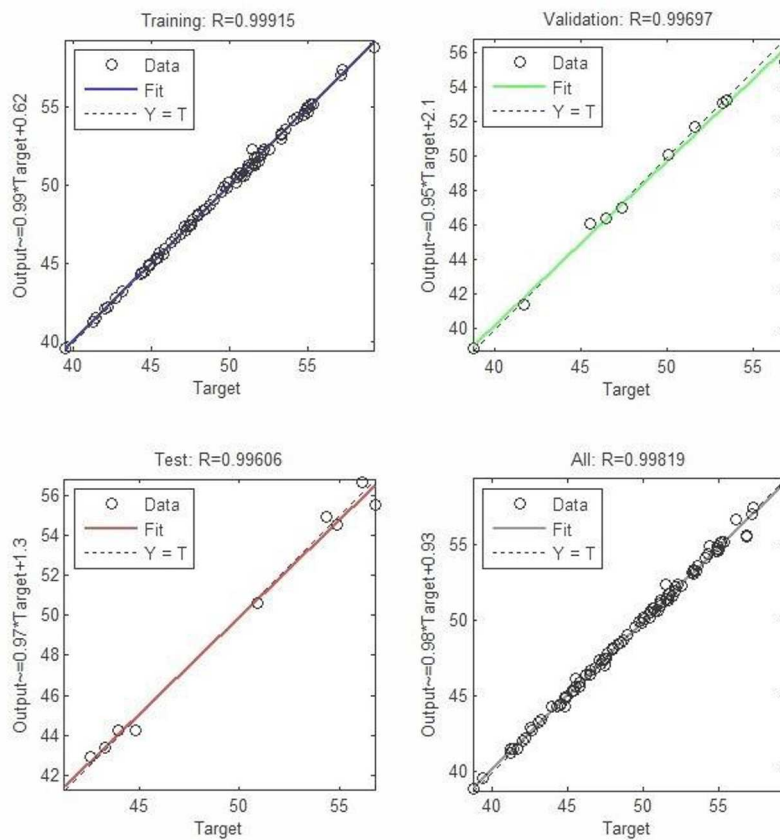
Increasing factor  $\mu$ : 10  
 Maximum time: Inf



(a)

Figure 6: (a). For the legend see next page.

Regression analysis plot of training, validation and testing are all shown in Fig. 6 for both types of collector. From Fig. 6(a), it is found that the values of  $R$  of unidirectional flow collector in training time, validation, testing and all time are 0.99979, 0.99959, 0.99885, and 0.99971, respectively. Similarly from Fig. 6(b), for cross flow type the values of  $R$  in training; validation testing and all period are 0.99915, 0.99697, 0.99606, and 0.99819, respectively. Based on these results, it is concluded that MLP structure



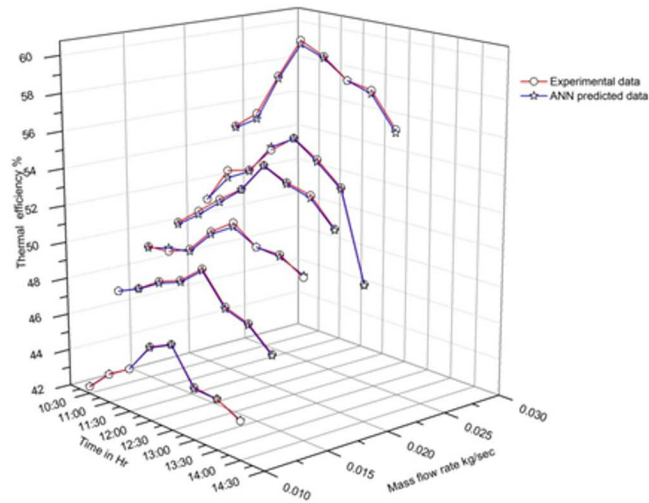
(b)

Figure 6: Regression analysis plot of solar air heaters with training, validation, testing and all data for LM-13: (a) – unidirectional flow, (b) – cross flow.

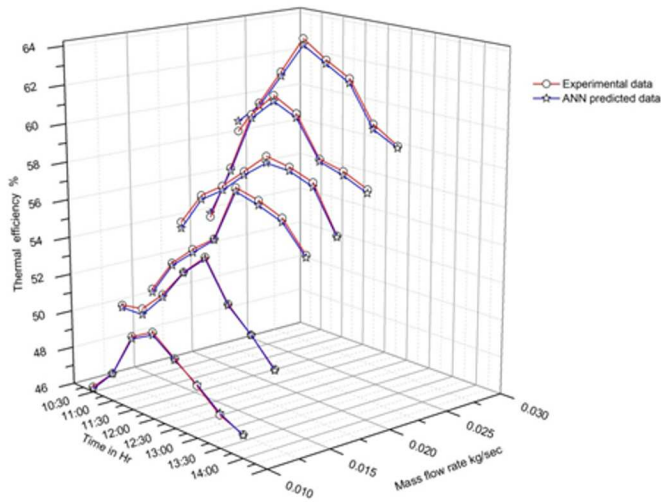
of ANN can be used for solar collectors very well to predict its thermal performance.

The comparison between actual (experimental) data and predicted (ANN) data of thermal efficiency for unidirectional porous bed solar air heater with respect to time and mass flow rate has been shown in Fig. 7(a) for type **A** and in 7(b) for type **B** of screen -absorbers. For the cross flow type, it has been shown in Fig. 8(a) and 8(b), respectively.

For selected MLP with LM-13, ANN predicted thermal performance of porous bed solar air heater were evaluated by using the sum of squared



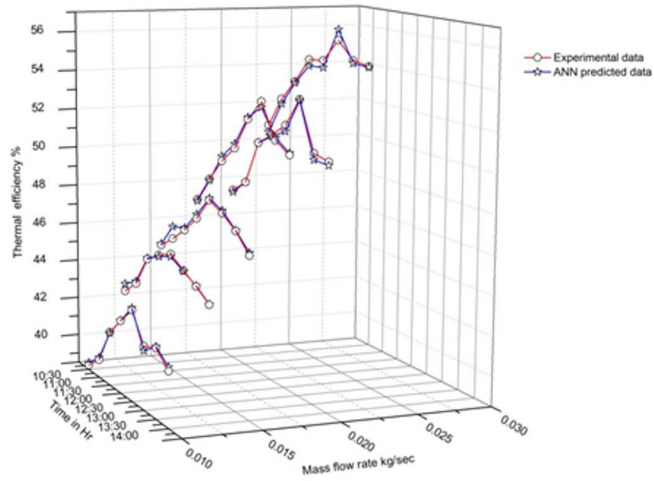
(a)



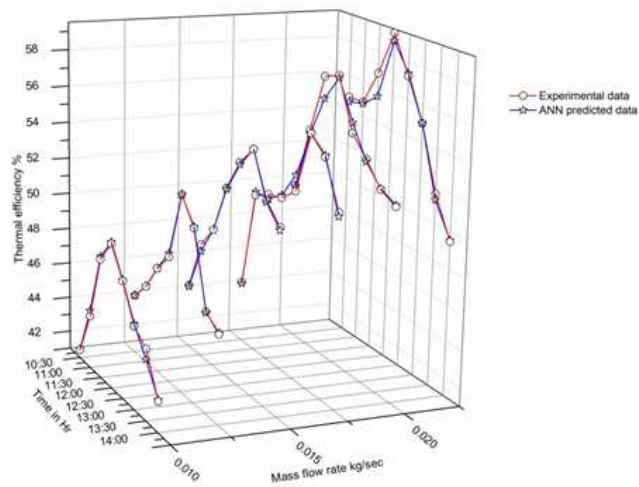
(b)

Figure 7: Comparison between experimental and ANN predicted thermal efficiency of unidirectional flow porous bed solar air heater for LM-13: (a) type **A**, (b) type **B**.





(a)



(b)

Figure 8: Comparison between experimental and ANN predicted thermal efficiency of cross flow porous bed solar air heater for LM-13: (a) type **A**, (b) type **B**.

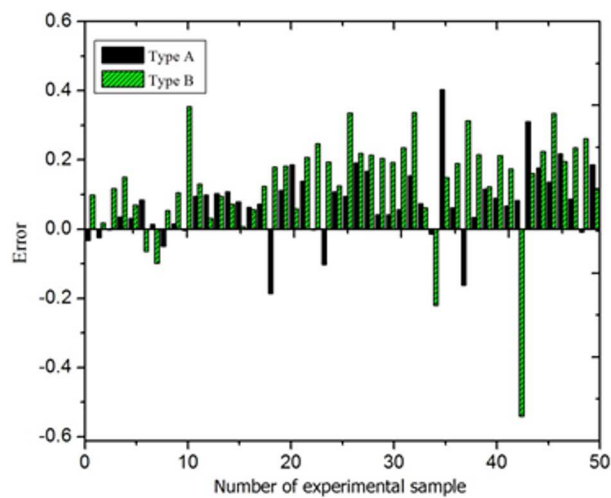


Figure 9: Individual error of unidirectional flow type collector.

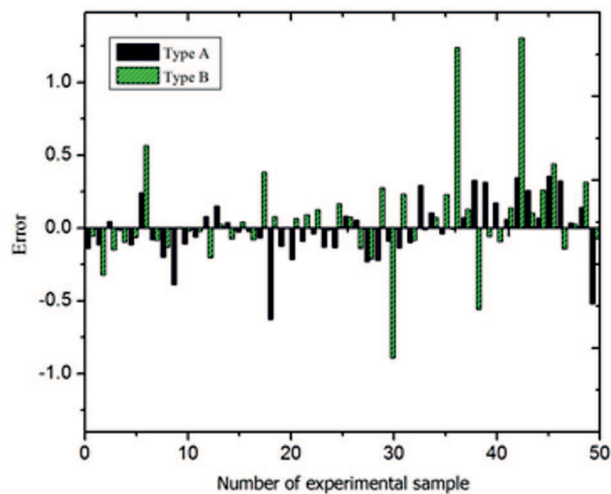


Figure 10: Individual error of cross flow type collector.

error (SSE), root mean square error (RMSE), coefficient of multiple determination ( $R^2$ ), mean relative error (MRE), coefficient of variance (COV) and mean absolute error (MAE). The performance prediction through the neural network is calculated by different types of errors [20,21] between the predicted and the actual data obtained from experiments as per the following expression:

mean absolute error

$$\text{MAE} = \frac{1}{n} \sum_{i=1}^n (X_{A,i} - Y_{P,i}), \quad (14)$$

sum of square error

$$\text{SSE} = \sum_{i=1}^n (X_{A,i} - Y_{P,i})^2, \quad (15)$$

root mean square error

$$\text{RMSE} = \sqrt{\frac{1}{n} \sum_{i=1}^n (X_{A,i} - Y_{P,i})^2}, \quad (16)$$

mean relative percent error

$$\text{MRE} = \frac{1}{n} \sum_{i=1}^n 100 \times \left( \frac{|X_{A,i} - Y_{P,i}|}{X_{A,i}} \right). \quad (17)$$

The absolute error is the absolute value of the deviation between actual values and estimated values (predicted values), which means individual error. The individual errors are shown as a bar chart in Figs. 9 and 10 of unidirectional and cross flow type porous bed solar air heaters, respectively. It is seen that most of errors in unidirectional type collector are between  $\pm 0.2$ , and in case of cross flow type collector the most of errors are between  $\pm 0.25$ . The mean absolute error, computed by using Eq. (14), for unidirectional flow of the proposed MLP is found as 0.10423. In case of cross flow it is found as 0.03428.

Here the MLP network represents nonlinear relationship between its inputs and outputs; it is trained to minimize a pre-specified error function. This training procedure essentially aims at obtaining an optimal set of network connection weights that minimizes a pre-specified error function. The widely utilized error function is known as root mean square error (RMSE) and RMSE minimization techniques is known as error back propagation

(EBP) algorithm. Root mean square error is calculated using Eq. (16). Using this equation RMSE value of the proposed unidirectional and cross flow networks is found as 0.16359 and 0.27693, respectively.

In statistical language  $R^2$  is called the coefficient of determination, which indicates the reliability of model. Higher value of  $R^2$  indicates more reliability of the model. The coefficient of determination is calculated using Eq. (11). The value of proposed network is found as 0.9994 and 0.9964 for both types of collector respectively.  $R^2$  ranges between 0 and 1. A very good fit yields  $R^2$  value of 1 or closer to 1, whereas a poor fit results to a value near 0. Mean relative errors are calculated using Eq. (17) and the MRE for both types of collector is 0.24676 and 0.36213, respectively.

Sum of squared error is calculated using Eq. (15). The SSE for proposed network for unidirectional and cross flow types collector is found as 1.35131 and 3.91871, respectively. In addition, coefficient of variance is calculated by Eq. (10), for both types and there values are obtained as 0.30515 and 0.56011, respectively. The histogram of the error of unidirectional and cross flow type collectors are shown in Figs. 11 and 12, respectively. It is seen that in unidirectional flow collector over 24% and 17% of the errors are accumulated for absorbers type **A** and type **B** across the values 0.05 to 0.075 and 0.16 to 0.2, respectively, and in case of cross flow collector over 22% and 17% of the errors are accumulated for type **A** and type **B** between -0.35 to -0.20 and -0.20 to -0.1, respectively. The comparison of error analysis results have been shown in Tabs. 4 and 5 for two different types of porous absorber, i.e., type **A** and type **B** for LM-13 respectively. It has been found that the value of  $R^2$  is closer to unity and remaining error values are very low which gives the satisfactory and accurate results of the selected ANN model.

Table 4: Performance of ANN model prediction of unidirectional flow collector.

	SSE	RMSE	MRE (%)	MAE	COV	$R^2$
Type <b>A</b>	0.76616	0.12633	0.18742	0.07385	0.24664	0.9995
Type <b>B</b>	1.93645	0.20085	0.30610	0.13462	0.36366	0.9991
Mean	1.35131	0.16359	0.24676	0.104235	0.30515	0.9994

The comparisons of present results with obtained by Caner *et al.* [25] ANN model are shown in Tab. 6. From Tab. 6, it can be said that results obtained by present model predicts optimal are accurate than Caner model.

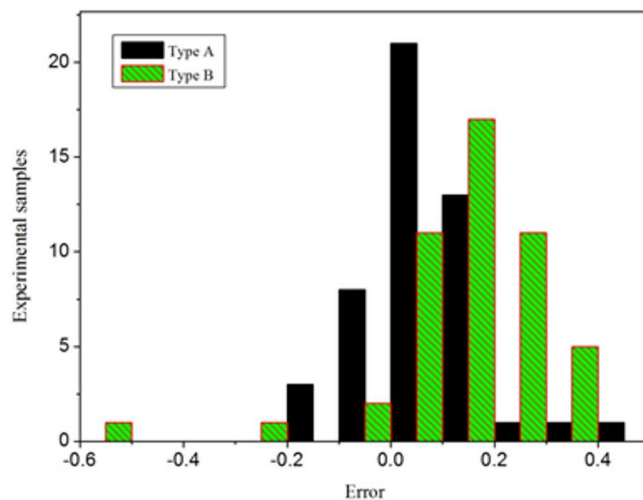


Figure 11: Histogram of errors of unidirectional flow collector.

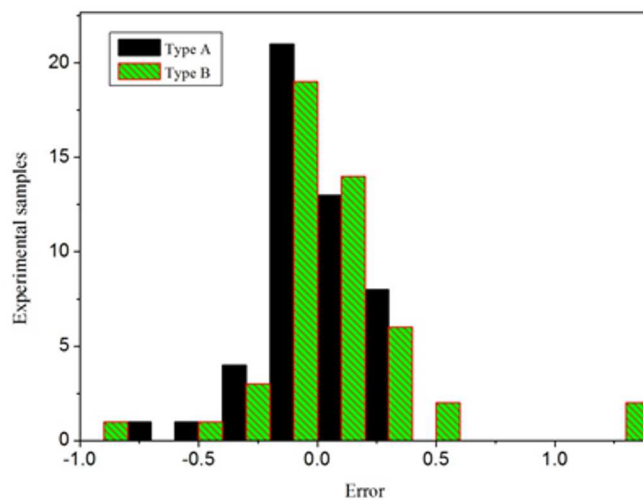


Figure 12: Histogram of errors of cross flow collector.

Table 5: Performance of ANN model prediction of cross flow collector.

	SSE	RMSE	MRE (%)	MAE	COV	$R^2$
Type <b>A</b>	2.04890	0.20660	0.32542	0.01057	0.43040	0.9989
Type <b>B</b>	5.78852	0.34726	0.39885	0.05799	0.68982	0.9939
Mean	3.91871	0.27693	0.36213	0.03428	0.56011	0.9964

Table 6: The comparisons of previous and present work.

Literature	Statistical Results			
	Type	$R^2$	MAE	MRE
Caner <i>et al.</i> [25]	<b>A</b>	0.9984	0.9204	2.5549
	<b>B</b>	0.9994	1.0554	3.5793
Present work	<b>A</b>	0.9994	0.1042	0.2467
	<b>B</b>	0.9964	0.0342	0.3621

## 4 Conclusions

In present work, the effectiveness of unidirectional flow and cross flow types porous bed solar air heaters (SAHs) have been experimentally determined and compared. The Artificial Neural Networks (ANN) technique has also been applied to predict the effectiveness of these two SAHs. The analysis has been carried out for mass flow rates from 0.0100 kg/s to 0.0225 kg/s. The ANN structure has been constructed with MLP model, using seven parameters in input layer and one parameter in output layer. The experimental results have been compared with those of ANN predicted values. On basis of the experimental results and ANN predicted results, the following conclusions have been drawn:

1. The effectiveness for unidirectional flow porous bed SAH is 55.1% and that of cross flow type is 50.93% for type **B** absorber at air mass flow rate of 0.0225 kg/s.
2. The effectiveness of unidirectional flow SAH at mass flow rate of 0.0225 kg/s is 7.45% higher, whereas at mass flow rate of 0.0100 kg/s it is 9.40% higher than the cross flow type SAH for type **A** absorber.

Thus unirectional flow porous bed SAH is more effective than cross flow type.

3. For most optimal topology the number of neurons in hidden layer are found to be thirteen (LM-13) for both types of solar air heaters.
4. For predicted effectiveness,  $R^2$  values in Levenberg-Marquardt (LM) algorithms are found to be 0.9994 and 0.9964 for unidirectional flow and cross flow solar air heaters respectively which are close to unity and are acceptable.
5. The values of root mean square error, mean relative error and coefficient of variance for unidirectional flow are 0.16359, 0.24676, and 0.30515, respectively, where as, for cross flow type these are 0.27693, 0.36213 and 0.56011 respectively which are lower as desired.
6. The result of the ANN model is accurate and satisfactory with the experimental data.
7. A larger database inputs used as training sets of data in neural network model may further improve the predictions. The ANN model developed can predict fast and accurate results of thermal efficiency of porous bed solar air heater. ANN technique can be used in several engineering applications as it provides better, quick and more realistic results without the need of conducting series of tests for a long time.

Received 28 November 2017

## References

- [1] DUFFIE J.A., BECKMAN W.A.: *Solar Engineering of Thermal Processes* (2nd Edn.). Wiley, New York 1991.
- [2] TIWARI G.N.: *Solar Energy: Fundamentals, Design, Modelling and Applications*. Narosa, New Delhi 2004.
- [3] KARSLI S.: *Performance analysis of new-design solar air collectors for drying applications*. *Renew. Energy* **32**(2007) 1645–1660.
- [4] PRASAD B.N., BEHURA A.K., PRASAD L.: *Fluid flow and heat transfer analysis for heat transfer enhancement in three sided artificially roughened solar air heater*. *Sol. Energy* **105**(2014), 27–35.

- [5] BEHURA A.K., PRASAD B.N., PRASAD L.: *Heat transfer, friction factor and thermal performance of three sides artificially roughened solar air heaters*. Sol. Energy **130**(2016), 46–59.
- [6] BEHURA A.K., ROUT S.K., PANDYA H., KUMAR A.: *Thermal analysis of three sides artificially roughened solar air heaters*. Energy Procedia **109**(2017) 279–285.
- [7] SHARMA S.P., SAINI J.S., VARMA H.K.: *Thermal performance of packed bed solar air heaters*. Sol. Energy **47**(1991) 59–67.
- [8] PRASAD R.K., SAINI, J.S.: *Comparative performance study of packed bed solar air heaters*. In: Proc. 8th ISME Conf. on Mechanical Engineering, New Delhi, 1993, 190–197
- [9] Prasad R.K., Saini J.S.: *Thermal performance characteristics of unidirectional flow porous bed solar energy collectors for heating air*. PhD thesis, University of Roorkee, Roorkee 1993.
- [10] AHMAD A., SAINI J.S., VARMA H.K.: *Effect of geometrical and thermophysical characteristics of bed materials on the enhancement of thermal performance of packed bed solar air heaters*. Energy Conv. Mgmt. **36**(1995), 1185–1195.
- [11] VARSHNEY L., SAINI J.S.: *Heat transfer and friction factor correlations for rectangular solar air heater duct packed with wire mesh screen matrices*. Sol. Energy **62**(1998), 4, 255–262.
- [12] THAKUR N.S., SAINI J.S., SOLANKI S.C.: *Heat transfer and friction factor correlations for packed bed solar air heater for a low porosity system*. Sol. Energy **74**(2003), 319–329.
- [13] MITTAL M.K., VARSHNEY L.: *Optimal thermohydraulic performance of a wire mesh packed solar air heater*. Sol. Energy **80**(2006), 1112–1120.
- [14] A.P. Omojaro, L.B.Y. Aldabbagh: *Experimental performance of single and double pass solar air heater with fins and steel wire mesh as absorber*. Appl. Energ. **87**(2010), 3759–3765.
- [15] KALOGIROU S.A.: *Applications of artificial neural-networks for energy systems*. Appl. Energ. **67**(2000), 1-2, 17–35.
- [16] KALOGIROU S.A., BOJIC M.: *Artificial neural networks for the prediction of the energy consumption of a passive solar building*. Energy **25**(2000), 479–491.
- [17] YANG I.H., YEO M.S., KIM K.W.: *Application of artificial neural network to predict the optimal start time for heating system in building*. Energ. Convers. Manage. **44**(2003), 2791–2809.
- [18] FACAO J., VARGA S., OLIVEIRA A.C.: *Evaluation of the Use of Artificial Neural Networks for the Simulation of Hybrid Solar Collectors*. Int. J. Green Energy **1**(2004), 3, 337–352.
- [19] ERTUNC H.M., HOSOZ M.: *Artificial neural network analysis of a refrigeration system with an evaporative condenser*. Appl. Therm. Eng. **26**(2006), 627–635.
- [20] KALOGIROU S.A.: *Prediction of flat-plate collector performance parameters using artificial neural networks*. Sol. Energy **80**(2006), 248–259.
- [21] YILMAZ S., ATIK K.: *Modeling of a mechanical cooling system with variable cooling capacity by using artificial neural network*. Appl. Therm. Eng. **27**(2007), 2308–2313.



- [22] SOZEN A., MENLIK T., UNVAR S.: *Determination of efficiency of flat-plate solar collectors using neural network approach*. Expert Syst. Appl. **35**(2008), 4, 1533–1539.
- [23] KURT H., ATIK K., OZKAYMAK M., RECEBLI Z.: *Thermal performance parameters estimation of hot box type solar cooker by using artificial neural network*. Int. J. Therm. Sci. **47**(2008), 192–200.
- [24] YUHONG Z., WENXIN H.: *Application of artificial neural network to predict the friction factor of open channel flow*. Commun. Nonlinear Sci. **14**(2009), 5, 2373–2378.
- [25] CANER M., GEDIK E., KECEBAS A.: *Investigation on thermal performance calculation of two type solar air collectors using artificial neural network*. Expert Syst. Appl. **38**(2011), 3, 1668–1674.
- [26] BENLI H.: *Determination of thermal performance calculation of two different types solar air collectors with the use of artificial neural networks*. Int. J. Heat Mass Tran. **60**(2013), 1–7.
- [27] DIKMEN E., AYAZ M., EZEN H.S., KUCUKSILLE E.U., SAHIN A.S.: *Estimation and optimization of thermal performance of evacuated tube solar collector system*. Heat Mass Transfer **50**(2014), 5, 711–719.
- [28] KALOGIROU S.A., MATHIOULAKIS E., BELESSIOTIS V.: *Artificial neural networks for the performance prediction of large solar systems*. Renew. Energy **63**(2014), 90–97.
- [29] GHRITLAHRE H.K., PRASAD R.K.: *Prediction of thermal performance of unidirectional flow porous bed solar air heater with optimal training function using artificial neural network*. Energy Procedia **109**(2017), 369–376.
- [30] HAYKIN S.: *Neural Networks. A Comprehensive Foundation*. Prentice-Hall, New Jersey 1994.
- [31] MAY R.J., MAIER H.R., DANDY G.C., FERNANDO T.M.K.G.: *Non-linear variable selection for artificial neural networks using partial mutual information*. Environ. Modell. Softw. **23**(2008), 1312–1326.
- [32] MAY R., DANDY G., MAIER H.: *Review of input variable selection methods for artificial neural networks*. In: Artificial neural networks-methodological advances and biomedical applications (S. Kenji, ed.), InTech, Rijeka 2011.
- [33] GHRITLAHRE H.K., PRASAD R.K.: *Energetic and exergetic performance prediction of roughened solar air heater using artificial neural network*. Ciencia e Tecnica Vitivinicola **32**(2017), 11, 2–24.
- [34] GHRITLAHRE H.K., PRASAD R.K.: *Application of ANN technique to predict the performance of solar collector systems – A review*. Renew. Sust. Energ. Rev. **84**(2018) 75–88.
- [35] GHRITLAHRE H.K., PRASAD R.K.: *Development of optimal ANN model to estimate the thermal performance of roughened solar air heater using two different learning algorithms*. Annals of Data Sci. (2018), 1–15.
- [36] GHRITLAHRE H.K., PRASAD R.K.: *Energetic performance prediction of a roughened solar air heater using artificial neural network*. Strojnicki vestnik – J. Mech. Eng. **64**(2018), 3, 195–206.

- [37] GHRITLAHRE H.K., PRASAD R.K.: *Investigation on heat transfer characteristics of roughened solar air heater using ANN technique*. Int. J. Heat Technology **36**(2018), 1, 102–110.
- [38] GHRITLAHRE H.K., PRASAD R.K.: *Investigation of thermal performance of unidirectional flow porous bed solar air heater using MLP, GRNN, and RBF models of ANN technique*. Therm. Sci. Eng. Prog. **6**(2018), 226–235.
- [39] GHRITLAHRE H.K., PRASAD R.K.: *Energetic performance prediction of solar air heater using MLP, GRNN and RBF models of artificial neural network technique*. J. Environ. Manage. **223**(2018), 566–575.
- [40] Matlab, Version 8.4, Neural Network Tool Box, Inc. R2014b.